Eur. Phys. J. A (2012) **48**: 85
DOI 10.1140/epja/i2012-12085-6

THE EUROPEAN PHYSICAL JOURNAL A

Special Article – Tools for Experiment and Theory

T-REX

A new setup for transfer experiments at REX-ISOLDE

Vinzenz Bildstein[1,a], Roman Gernhäuser[1], Thorsten Kröll[1,b], Reiner Krücken[1,c], Kathrin Wimmer[1,d], Piet Van Duppen[2], Mark Huyse[2], Nikolas Patronis[2,e], and Riccardo Raabe[2] for the T-REX Collaboration

[1] Physik Department E12, James-Franck-Straße, D-85748 Garching, Germany
[2] Instituut voor Kern- en Stralingsfysica, KU Leuven, Celestijnenlaan 200D, B-3001 Leuven, Belgium

Received: 19 December 2011 / Revised: 13 March 2012
Published online: 18 June 2012 – © Società Italiana di Fisica / Springer-Verlag 2012
Communicated by B.R. Fulton

Abstract. Transfer reactions in inverse kinematics using the radioactive ion beams provided by the REX-ISOLDE facility at CERN are very good tools to gain insight into the single-particle properties of exotic nuclei. The new silicon particle detector setup T-REX, optimized for these transfer reactions, is presented in this article. T-REX consists of position sensitive ΔE-E telescopes in a compact configuration that covers up to 66% of the solid angle. The setup allows the identification of the light reaction products and the measurement of their angular distribution for a large range of polar angles. Simultaneous detection of the elastically scattered target-like nuclei enables the determination of the optical model parameters used in the analysis of the experiments.

1 Introduction

Transfer reactions have been successfully used for decades to study the single-particle properties of nuclei close to the valley of stability. Usually the experiments were done with light beams (p, d, t, ^{3}He, α, etc.) impinging on heavy, stable targets, hence in "normal kinematics". The light beam-like ejectile is then detected in a spectrometer with a small solid angle but high resolution (*e.g.*, 5 keV for the Munich Q3D [1]).

With the advent of second- and third-generation radioactive beam facilities such as REX-ISOLDE [2] it became of interest to use the post-accelerated radioactive ion beams from ISOL[1] facilities for transfer reactions in "inverse kinematics", where the heavier beam hits the lighter target, to gain more insight on the single-particle properties of nuclei far from stability.

T-REX[2] is a new setup of silicon detectors, optimized for transfer reactions in inverse kinematics. It was designed to be used in combination with the MINIBALL γ-detector array [3], allowing the reconstruction of the excitation energy in the final nucleus with a better resolution than it could be obtained with particle spectroscopy alone. The setup is comparable with other devices such as TIARA [4,5], SHARC [6], and ORRUBA [7].

The first setup, including nearly all essential detectors and electronics, was tested with stable magnesium beam at the MLL[3] tandem laboratory in 2007. It was constantly improved through the years so that the setups differ in some details. In the following the setup of 2010 is presented with some references on the differences to the other setups.

Whole series of experiments with the new detector array have been performed at REX-ISOLDE, using one- and two-neutron transfer reactions and beams ranging from ^{11}Be to ^{78}Zn [8]. Experiments with beams heavier than $A = 80$ are at the time being limited by the achievable beam energies, see also sect. 10.

2 REX-ISOLDE

The radioactive ion beams are produced at ISOLDE [9] by impinging a high-energy proton beam (1.4 GeV) on

[a] *Present address*: Department of Physics, University of Guelph, Guelph, Ontario, Canada N1G 2W1; e-mail: vbildste@uoguelph.ca
[b] *Present address*: Institut für Kernphysik, TU Darmstadt, Schlossgartenstraße 9, D-64289 Darmstadt, Germany.
[c] *Present address*: TRIUMF, 4004 Wesbrook Mall, Vancouver, BC, Canada V6T 2A3.
[d] *Present address*: National Superconducting Cyclotron Laboratory, 1 Cyclotron, East Lansing, Michigan 48824-1321, USA.
[e] *Present address*: Department of Physics, The University of Ioannina, GR-45110 Ioannina, Greece.
[1] Isotope Separation On-Line.
[2] Transfer at REX.
[3] Maier-Leibnitz-Laboratorium der Universität und der Technischen Universität München, Am Coulombwall 6, 85748 Garching, Germany.

a thick, heavy target, *e.g.*, 50 g cm^{-2} Uranium carbide [10]. The resulting radioactive ions are ionized, extracted and mass separated. The singly charged ions are collected in the REX-TRAP, charge bred to a higher charge state in the REX-EBIS and post-accelerated by the REX-LINAC to energies up to 3 MeV u^{-1}.

Due to the spill structure of the REX beams (bunches of a few hundred μs length at maximal 50 Hz), the instantaneous rate can be high despite the relatively low average beam intensities so that no standard techniques can be used for beam monitoring, see subsect. 5.4.

The spill structure of the beam is also used for the data acquisition. The electronics modules buffer all events that fall into a 800 μs so-called on-beam window triggered by the REX-EBIS. After the data has been read-out from the modules (which takes about 4 ms to 7 ms), another so-called off-beam window of the same length is opened to acquire data without beam as a background reference (see also [11]). Timestamps generated for signals from both HPGe and silicon detectors allow to reconstruct the detected events.

3 Transfer reactions

The main aim of T-REX is to measure (d,p) and (t,p) transfer reactions with radioactive beams. This requires the identification and measurement of the protons from said reactions as well as the target-like recoils from (d,d) and (t,t) reactions. The latter is important as the simultaneous measurement of the elastically scattered recoils allows the optical model parameters used for the DWBA calculations of the angular distribution of the protons from the transfer reaction to be constrained. The measurement of the elastically scattered recoils also provides the means to determine the beam luminosity thus giving an overall normalization.

The target used for (d,p) reactions is a deuterated polyethylene foil of 100 μg cm^{-2} or 1 mg cm^{-2} thickness. For the (t,p) reaction a tritium loaded titanium foil is being used which is 500 μg cm^{-2} thick and contains about 40 μg cm^{-2} tritium. This target has an activity of 10 GBq.

These targets always contain some protons as well (on the level of a few %), thus allowing to determine the optical model parameters for elastically scattered protons as well.

Figure 1 shows the typical kinematics of a transfer reaction in inverse kinematics. Depicted is the relation between energy and scattering angle in the laboratory frame for the d(^{66}Ni, p)^{67}Ni reaction. The calculation is done for a thick (1 mg cm^{-2}) deuterated polyethylene target, assuming that the reaction takes place at the middle of the target. It includes the energy loss of the beam in the first half of the target and the energy loss of the recoils generated at the center of the target as well as the energy loss in the protective foils in front of the forward detectors. Also included in the figure are the energy loss in the ΔE detectors used in the standard T-REX setup.

The experiments performed with T-REX so far are

- 2007: first d(^{30}Mg, p)^{31}Mg.

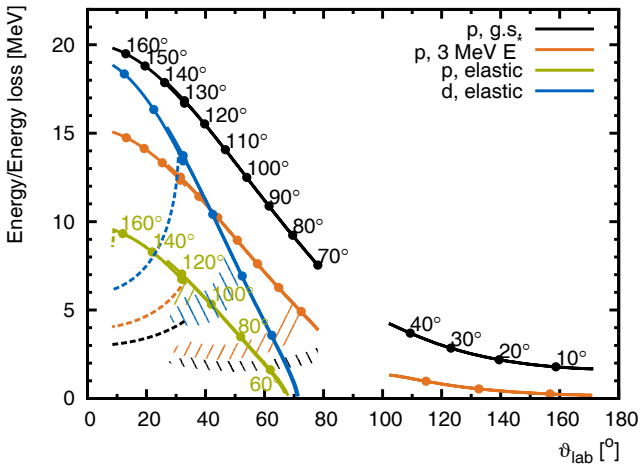


Fig. 1. The solid lines show the energy *vs.* ϑ_{lab} relation for protons from the d(^{66}Ni, p)^{67}Ni reaction at 2.9 MeV u^{-1} as well as elastically scattered protons and deuterons. The hashed areas and dashed lines show the energy deposited by the particles in the ΔE detectors. The energy deposited in the barrel detectors (sect. 5) is shown as an area since the effective thickness of the detectors depends not only on ϑ_{lab} but also on φ. ϑ_{cm} angles are indicated along the kinematic lines as dots.

- 2008: t(^{30}Mg, p)^{32}Mg [12] and second d(^{30}Mg, p)^{31}Mg [13].
- 2009: transfer reactions with ^{11}Be beam and d(^{66}Ni, p)^{67}Ni.
- 2010: transfer reactions with ^{11}Be beam, t(^{44}Ar, p)^{46}Ar, and d(^{78}Zn, p)^{79}Zn.
- 2011: t(^{66}Ni, p)^{68}Ni and t(^{72}Zn, p)^{74}Zn.

4 Design parameters

The inverse kinematics and the use of radioactive beams impose six main requirements on the experimental setup (see also fig. 1).

Angular coverage: in inverse kinematics the small polar angles of the beam-like ejectiles require the measurement of the recoils (so far, in most cases protons) for a wide range of polar angles.

Solid angle coverage: the low intensity of the radioactive beams and the limited beam time available require a highly efficient setup that covers a large solid angle.

Particle identification: particle identification is necessary to identify the light reaction products and in order to suppress background created by electrons/positrons from the β-decay of stopped radioactive beam particles.

Angular resolution: a reasonable resolution of the polar angles is necessary to probe the angular distribution of the transfer reactions and to reduce the kinematic broadening of the excitation energy resolution (see also sect. 8).

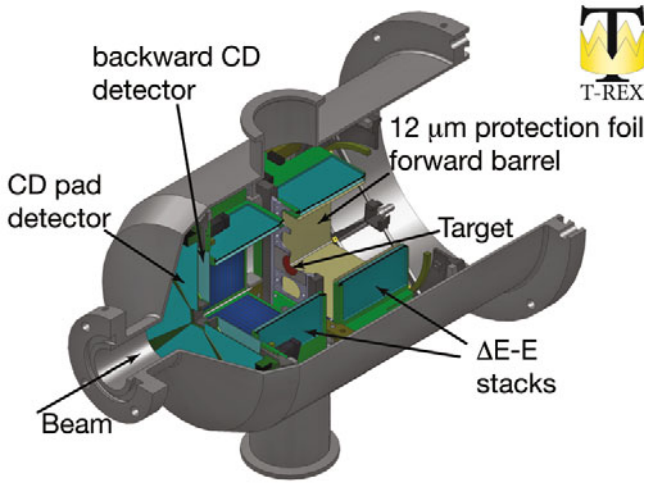


Fig. 2. Engineering drawing of the silicon barrel inside the vacuum chamber as it was used in 2010 with barrel and backward CD detectors.

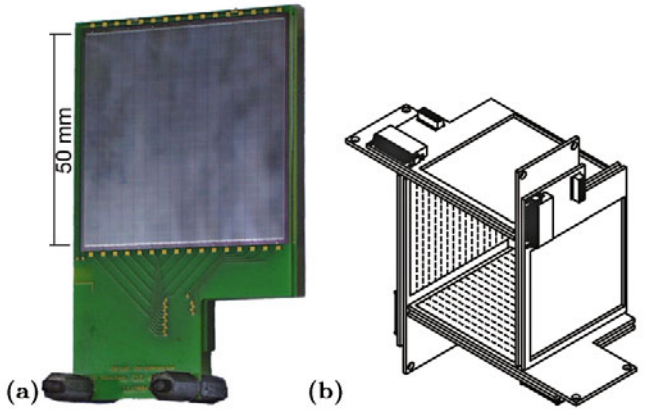


Fig. 3. (a) The PCB packaging of the barrel detectors. The 140 μm thick ΔE detectors are segmented into 16 vertical resistive strips. The E detectors are hidden behind, in the picture. (b) Four units are assembled in a windmill shape, with the segmentation indicated by dashed lines.

Compact setup: the setup has to be as compact as possible not to decrease the γ-ray detection efficiency of the surrounding MINIBALL γ-detector array.

Low material budget: in order to limit the attenuation of γ-rays the amount of material used in the construction of T-REX has to be limited.

In order to minimize background from the β-decay of stopped beam particles the amount of material in the beam line has to be minimized to reduce the elastic scattering of the beam. This puts constraints on the target thickness as well as the thickness of any beam monitors (see subsect. 5.4).

5 Implementation

In order to fulfill all the requirements, a design consisting of position sensitive ΔE-E telescopes of silicon detectors was chosen. The detectors are arranged around the target, separated in two halves pointing in forward and backward direction as shown in fig. 2, with a gap at 90° for the target holder.

To limit the number of electronic readout channels it was decided to use RSSDs[4] with minimal segmentation to cover the angles closest to 90°, while the very forward and/or backward angles are covered by DSSSDs[5]. The use of RSSDs has the additional advantage of reducing the amount of cables inside the chamber, the number of feedthroughs and the amount of electronics needed.

5.1 Mechanical layout

To optimize the solid angle covered by the particle detectors (*i.e.* ϑ_{lab} and φ), T-REX consists of two boxes of RSSDs (the barrel detectors), one on either side of $\vartheta_{\mathrm{lab}} = 90°$, and includes one or two DSSSDs in the shape of a compact disc (CD detectors) [14] up- and/or downstream. The solid angle covered by the barrel detectors is about 56% of 4π and the CD detectors cover an additional 10%, leading to a total coverage of about 66% of 4π. To maximize the coverage of azimuthal angles, the barrel detectors are arranged in a windmill shape with the connectors outside the boxes (see fig. 3b).

Furthermore the position-sensitive strips, which measure the position along the strip by splitting the deposited charge, are oriented perpendicular to the beam and only one end is read out, the other ends of all strips are connected and only used to apply high voltage to the detector. This allows to have no PCB on one side of the detector and only a very small strip on the other, thus optimizing the coverage of polar angles (*i.e.* ϑ_{lab}).

In the current setup the windmill configuration was chosen such that there is no PCB between the barrel detectors and the CD detectors, minimizing the gap around 30°/150° while increasing the gap around 90°. This could be changed by using an inverted windmill configuration to cover angles closer to 90°.

The barrel detectors are placed at a distance of 29 mm from the beam axis, resulting in the same coverage of azimuthal angles as for the CD detectors (about 90%).

The targets are mounted on a target ladder that can hold up to 4 targets and is inserted between the two halves of the barrel by a magnetically coupled linear feedthrough. Two different target ladder designs are used, either with an extra mounting for the 9-fold segmented diamond detector for beam focusing or with a special 4th target position suited for tritium loaded titanium foils. This target position is sealed air tight in the retracted position to provide an extra radiation safety precaution.

Since 2009 two different guiding rails can be installed for the two different target ladder designs which ensure the exact positioning of the target in both horizontal directions (see fig. 4a). The vertical alignment of the target

[4] Resistive-Strip Silicon Detector.
[5] Double-Sided Silicon-Strip Detector.

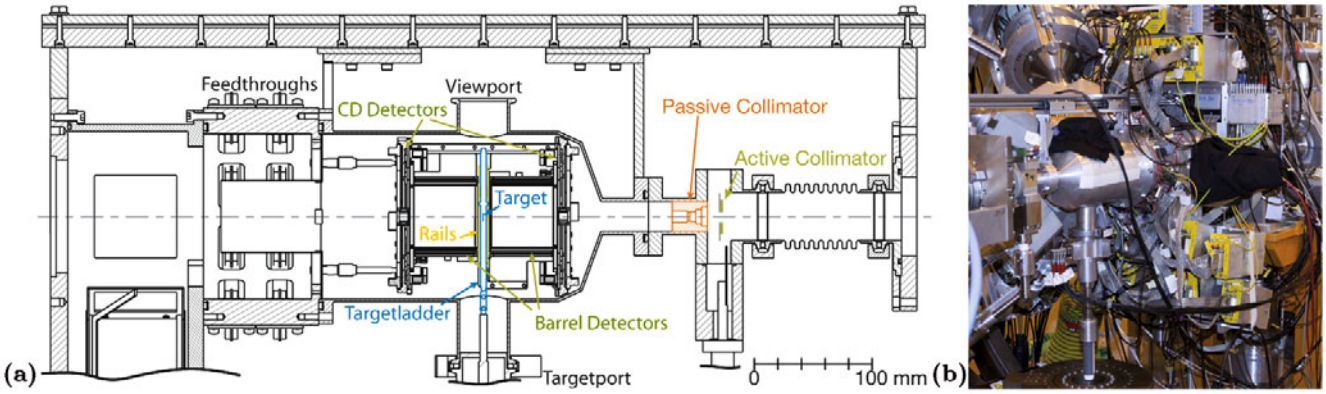


Fig. 4. The technical drawing of the T-REX setup, beam entering from the right (a) and a picture of the T-REX setup with one half of the MINIBALL array opened, beam entering from the left (b).

is ensured by the usage of spacers made for each target ladder design and target position.

In order to create an economic, compact, and flexible technique to lead up to 800 read out channels from vacuum to air, new feedthroughs were designed. These feedthroughs are made of stainless steel and any PCB with a width of 23 mm can be glued into them. The design of the feedthroughs, with a larger block that holds the PCB and is surrounded by a groove, ensures the decoupling of the mechanical forces of the sealing from the PCB-steel bond. In the current design one feedthrough is needed for each quadrant of the barrel detectors (forward and backward detector share one feedthrough). The CD detectors need one additional feedthrough each as well as two feedthroughs for all CD pad detectors. This means that currently 14 out of the 16 feedthroughs are used, leaving two for future additional detectors.

The target chamber for T-REX has an inner diameter of 140 mm and a wall thickness of 2 mm. The photopeak efficiency of MINIBALL is 5.0(3)% at 1332 keV in the T-REX configuration.

5.2 Detectors

To identify the light reaction products at low energies the ΔE detectors should be as thin as possible. However, for very thin detectors the large capacitance of the unsegmented rear introduces substantial electronic noise and the mechanical stability of the detectors is reduced. Also for particles at higher energies a certain thickness of the ΔE detectors is required so that the energy deposited in these detectors is above the detection threshold and well separated from the noise. The thickness chosen for the barrel ΔE detectors is 140 μm. This results in an identification of protons above 5 MeV to 7 MeV (depending on the impact angle), while the energy deposited by higher energetic protons ($\approx$ 20 MeV) is about 600 keV, hence well above the trigger threshold for the ΔE detectors (see also figs. 1 and 5).

The RSSDs are of the design X1 from Micron Semiconductors with the above mentioned thickness of 140 μm and an active area of 50 mm $\times$ 50 mm. They are segmented

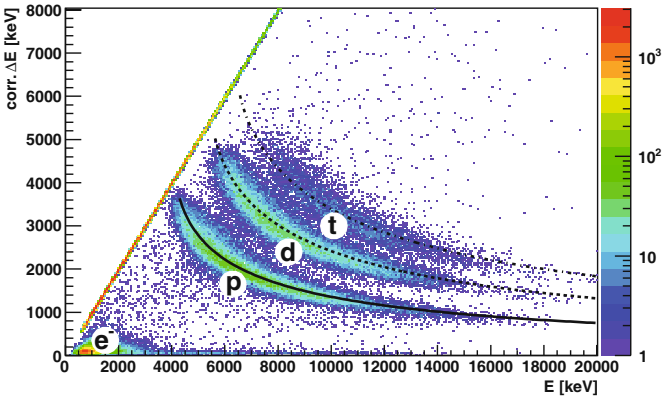


Fig. 5. ΔE-$E_{\mathrm{tot.}}$ particle identification in the forward barrel detectors for reaction products from the d(^{30}Mg, p)^{31}Mg reaction at 2.85 MeV u^{-1}. Protons (solid), deuterons (dashed) and tritons (dash-dotted) from reactions of ^{30}Mg with a 1 mg cm^{-2} deuterated polyethylene target can be clearly distinguished, as well as electrons from β-decay (lower left corner). The energy loss was corrected for the effective thickness of the ΔE detectors at the different angles of the impinging particles ($\approx$ 30° to 75°).

into 16 resistive strips and therefore provide a position resolution along the strip obtained from the comparison of the signal of one end of the strip and the back plane energy. The position resolution along the strip is better than the segmentation of 3.125 mm, even for low-energy particles (few hundred keV protons). For alpha particles at about 5 MeV a position resolution of about 0.1 mm can be achieved. The decision to arrange the strips perpendicular to the beam is thus not optimal for the ϑ_{lab} resolution but allows to cover a larger ϑ_{lab} range. The E detectors of the ΔE-E telescopes are made out of 1 mm thick pad detectors from Canberra (design RF) and are mounted 2.2 mm behind the ΔE detectors. This allows the detection of the full energy of protons with up to 20 MeV at a scattering angle of $\vartheta_{\mathrm{lab}} = 30°$.

The very forward and/or backward angles can be covered by CD detectors, each consisting of four quadrants of

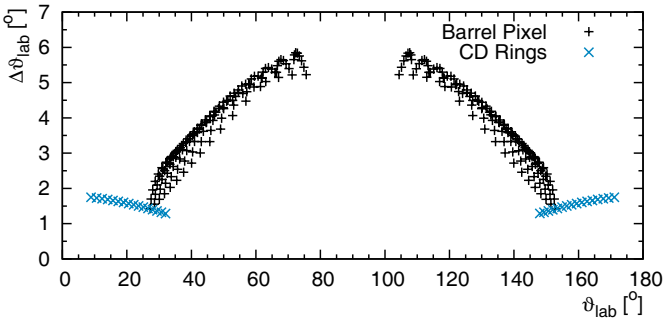


Fig. 6. Polar resolution achievable with T-REX if the strips are divided in the analysis into 16 bins along their length.

the standard DSSSD (Design QQQ2 from Micron Semiconductors [15]) with annular segmentation on the front and radial segmentation on the back. The detectors are backed by unsegmented CD quadrants as E detectors (Design QQQ1 from Micron Semiconductors). This combination is the same that is also used for all Coulomb excitation experiments with MINIBALL. In the 2010 setup only one such ΔE-E combination existed with both detectors of the same thickness of 500 μm, which was used in either forward or backward direction.

The relatively low segmentation of the barrel detectors is reflected in the lower polar angle resolution around 90° as can be seen in fig. 6. However, the polar angle resolution achievable with T-REX is sufficient to determine the angular distributions of transfer reactions. The additional kinematic broadening is usually similar to the uncertainty introduced by the target thickness (table 2). The kinematic compression, *i.e.* the fact that a 1 MeV difference in excitation energy translates into only 300 keV to 500 keV difference in the kinematic energy of the protons in backward direction, is an additional challenge in transfer reactions in inverse kinematics. This, combined with the energy broadening, requires in most cases the use of the MINIBALL array to identify the populated states by their characteristic γ-rays.

Table 1 gives an overview of the detectors currently available for use with the T-REX setup. In the setups from 2007 to 2010 the 500 μm thick segmented and unsegmented CD detectors were used together, either in forward (transfer experiments with ^{11}Be beam) or backward (all other experiments before 2011) direction. Since 2011 the segmented CD detectors with 140 μm thickness are used in backward direction together with the 500 μm thick unsegmented CD detectors. The combination of segmented CD detectors with 500 μm thickness with the 1500 μm thick unsegmented CD detectors is used in forward direction.

The 500 μm thick RSSDs are mounted on a single PCB each, without any backing E detector and are used in a different configuration of the particle detector setup to perform Coulomb excitation experiments.

5.3 Foils

To protect the silicon detectors from high rates of elastically scattered particles there are four different places in the setup to put foils in front of them. Starting from the most forward angles, a foil can be placed a few millimeters in front of a possible forward CD detector to stop any elastically scattered beam from reaching the detectors (thickness $\approx 50\,\mu$m of Mylar^{TM}[6]).

Since most beams used at REX-ISOLDE are substantially heavier than the heaviest constituent of a polyethylene target (^{12}C), elastically scattered beam is no problem for the barrel detectors but recoiling ^{12}C or deuterons emitted close to $\vartheta_{cm} = 0°$ are detected around $\vartheta_{lab} = 90°$ and could thus pose a rate and/or dead-time problem as well as damage the detectors. To reduce the number of elastically scattered recoils hitting the barrel detectors a typically 12 μm thick Mylar^{TM} foil can be mounted 2 mm in front of the barrel detectors. Such a foil stops elastically scattered carbon and deuterons, preventing them from hitting the strip of the barrel detectors closest to $\vartheta_{lab} = 90°$ which corresponds to a $\vartheta_{cm} \approx 15°$ to 30°. This way most of the carbons and deuterons, which would hit the barrel detectors, are stopped, and the ϑ_{cm} range, in which the elastically scattered deuterons can be used to determine the optical potential, is not too severely reduced.

If the beam used is lighter than the heaviest target constituent, *e.g.*, if a tritium-loaded titanium foil is used as target for (t,p) experiments, back-scattering of the beam is possible. Since it is impossible to distinguish these back-scattered beam particles from the low-energy protons emitted in backward angles with a silicon ΔE-E stack, it is necessary to stop the back-scattered beam in a thin (typically 2 μm) Mylar^{TM} foil. Two different foils can be mounted in backward directions. One is placed a few millimeters in front of the target (with a hole in the middle to allow the beam to pass through) and protects primarily the backward barrel detectors. The second foil is placed directly in front of the backward CD detector in the same way as the thicker foil used to stop elastically scattered beam particles from reaching the forward CD detector.

5.4 Beam diagnostics

Due to the bunching of the quasi-continuous ISOLDE beam in the REX-TRAP and -EBIS, the instantaneous rate is a factor 100 to 1000 higher than the average beam intensity. Typically transfer experiments have used average beam intensities ranging from $10^4\,s^{-1}$ to $10^6\,s^{-1}$.

This combination of relatively low average beam intensity with high instantaneous rates makes the beam monitoring challenging. For this reason two additional detectors were integrated into the T-REX setup.

The first one is an "active collimator" consisting of four 10 mm × 10 mm PiN-diodes arranged symmetrically around a hole (⌀10 mm) which give an indication whether the beam is centered at the very entrance of the T-REX setup (see figs. 7a and 4a). This active collimator is located before a passive tungsten collimator as shown in fig. 4a. In order to protect the PiN-diodes during initial

[6] Bi-axially-oriented polyethylene terephthalate.

Table 1. Detector specifications. The 500 μm thick RSSDs can be used for Coulomb excitation experiments, whereas the ΔE-E combination of the 140 μm thick RSSDs with 1000 μm thick pad detectors is used for transfer experiments, making T-REX a very versatile device.

Detector type	Size	Segmentation	Thickness [μm]	Dead layer [nm]
Micron X1	50 mm × 50 mm	16 resistive strips	500	200
Micron X1	50 mm × 50 mm	16 resistive strips	140	200
Canberra RF	50 mm × 50 mm	–	1000	50
Micron QQQ2	9 mm to 41 mm, 81.6°	16 annular rings, 24 radial strips	140/500	700
Micron QQQ1	9 mm to 50 mm, 82°	–	500/1500	700

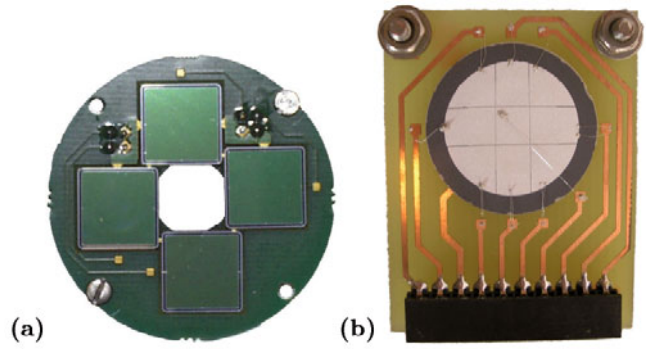


Fig. 7. The active collimator consisting of four 10 mm × 10 mm PiN-diodes (a) and the nine-fold segmented 10 μm thick diamond detector (with vacuum deposited titanium contacts, central segment is 3 mm × 3 mm) that can be inserted on the target position (b).

beam tuning, especially for high-intensity (stable) beams, an aperture can be introduced in the front of the active collimator, shielding the four PiN-diodes.

The second beam monitor that was integrated into the T-REX setup is a 10 μm thick nine-fold segmented polycrystalline CVD[7] diamond detector, as shown in fig. 7b. The central segment of the detector is 3 mm × 3 mm and the diameter is about 10 mm. The substrate material for this detectors is produced as a thin window on a silicon ring[8], while metalization (aluminum or titanium) and bonding was performed at the $E12$ target lab of the Technische Universität München. This diamond detector is thin enough not to stop any beam and can be mounted on the lowest position of the target ladder design so that the beam profile directly at the target position can be analyzed.

The individual readout of the signal generated by each particle impinging on the beam diagnostics detectors (especially the diamond detector) would require very fast electronics since the instantaneous beam rate can be very high (on the order of $10^{8-9}\,\mathrm{s}^{-1}$). But as long as it is not necessary to count each particle individually to see the position of the beam, the signals of the nine pixels of the diamond detector, its unsegmented rear side, and the four PiN diodes of the active collimator are integrated by a charge sensitive preamplifier without feedback resistor. The preamplifier integrates the charge over the length of one on- or off-beam time window and its output corresponds to the number of particles in the pulse plus the charge accumulated due to leaking currents. However, since the charge collecting properties of poly-crystalline diamond are not very good, it is impossible to get an absolute measurement of the beam intensity from the charge collected. At the end of the window an external fast reset signal is supplied via a photo-MOSFET.

The integrated signals of the beam diagnostics detectors are fed directly into an independent ADC which is gated by the on- and off-beam windows. The peak sensing of the ADC thus allows to measure the maximum charge accumulated in an on- and off-beam window, both of equal time, so that the charge accumulated in the preamplifiers due to leaking currents can be subtracted from the on-beam values.

5.5 Electronics

Each stack of ΔE-E barrel detectors is connected with one 26-fold flat ribbon cable to the feedthrough. It carries the signals from the 16 strips, the common signal from the other end of all 16 strips, and the rear side signal of the ΔE detector, as well as the front and rear side signals from the unsegmented E detector. On the outside of the chamber such cables also connect the feedthroughs and adapter PCBs, which are attached to MPR-16[9] preamplifiers. The adapter PCBs route the strip signals to the 25-pin SUB-D connectors of the MPR-16, filter the high voltage that is applied to the common side of the strips (which is not read out), and have two LEMO connectors to connect the ΔE and E signals to the MSI-8[9] preamplifier/shapers which also provide a fast "timing filter" output to externally generate trigger signals. The preamplified signals of the strips are amplified and shaped by STM-16[9] modules.

The negative bias is applied to the segmented front of the ΔE barrel detectors and the rear of the E barrel detectors.

32 channel VME ADCs MADC-32[9] are used for the digitization of the signals. To optimize the dead time of the system while keeping the number of ADCs needed low, the ADCs have been arranged in two independent

[7] Chemical Vapour Deposition.
[8] By Diamond Materials [16].
[9] From Mesytec [17].

so-called trigger groups of three ADCs each, one for the top and left detectors, and one for the bottom and right detectors. The trigger groups are gated by OR-ed triggers from the rear sides of the corresponding forward ΔE-E detectors, backward ΔE detectors and triggers of the two CD quadrants of the same group. The MADCs not only digitize the analog signals but also create timestamps for each gate, based on an external clock signal. This clock signal is also used for the timestamps of the XIA DGF modules reading the MINIBALL HPGe detectors, thus allowing to determine particle-γ coincidences.

The signals from the CD detectors are sent to MUX-16/-32[9] multiplexers. These multiplexers take 16 input signals and return for up to two of these the amplified and shaped signal as well as an analog signal coding the respective channel/strip number. Up to eight MUX-16 modules can be connected by one bus, so that only four signals are generated out of 128 input signals. If more than two input signals within one module are above the set threshold or if two modules on the same bus have input signals above threshold within 30 ns, the event is rejected and a corresponding reject signal is generated and fed into a scaler.

Since the rate in the CD detectors is low, it is expected that only one particle hits the CD within 30 ns, but this particle might create signals on up to two (neighboring) rings and strips due to charge sharing. Signals induced on neighboring channels by cross-talk are typically below the triggering threshold of the multiplexers and thus do no pose any problem. As only one module on the bus is allowed to have up to two hits at the same time, it is necessary to use different buses for the front (rings) and the rear (strips) side of the CD detector. The CD quadrants are connected corresponding to the trigger scheme of T-REX, with the front and rear sides of the CD quadrants on one bus each, for each the top and left, and the bottom and right quadrant, resulting in four buses, totaling an output of 16 analog signals for 128 channels.

6 Calibration

The energy calibration of the forward RSSD ΔE detectors is complicated because of the 12 μm Mylar^{TM} foils in front of them. While a normal mixed-nuclide α-source can still be used for the energy calibration, the energy loss of the α-particles in the foils has to be taken into account by comparing the data with either an energy loss calculation or a Geant4 simulation (see sect. 7).

The calibration of the E detectors has to be done in a different way, since these are situated behind the ΔE detectors and there is no practical way to calibrate them directly with an α-source. However, data taken with a ^{152}Eu or ^{60}Co γ-ray source to perform an efficiency and energy calibration of the surrounding MINIBALL γ-detector array can also be used to calibrate the E detectors. Some of the recorded events are a γ-ray that is Compton scattered in one of the E detectors and the Compton scattered γ-ray is then detected with its full energy in the MINIBALL array. These events can be used to calibrate the E detectors by gating on the anti-correlation between the (calibrated) energy of the MINIBALL array and E detectors as shown in fig. 8. A linear fit to this spectrum allows a very precise calibration of the silicon detectors with respect to the HPGe detectors, especially at low energies. Since this calibration is done with the electrons from the Compton scattering there are some uncertainties for the measurement of protons, deuterons, and tritons due to the different energy ranges (400 keV to 1200 keV for the electrons, 0 MeV to 25 MeV for protons, deuterons and tritons), different energy-losses in dead-layers, and the different ionization densities.

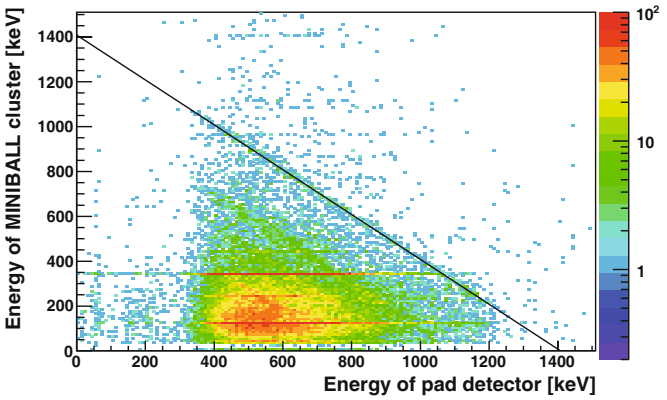


Fig. 8. The γ-ray energy detected with the MINIBALL array *versus* the energy in the E detectors for a ^{152}Eu source. One can clearly see the anti-correlation of the 1408 keV line, indicated with the black line. The spectrum also shows a trigger threshold of 350 keV for the E detectors.

Figure 8 also shows that a trigger threshold of 350 keV was achieved for the E detectors (energy full scale range of 15 MeV) whereas the threshold for the ΔE barrel detectors is normally around 500 keV (energy full scale range of 6 MeV).

To extend the calibration of the E detectors to higher energies, especially for the forward detectors where the energy deposited can be up to 25 MeV for tritons, the (pre-)calibrated ΔE-E spectra themselves can be used to calibrate the E detectors.

7 Simulation

This section describes the basic features of a Geant4 [18] Monte-Carlo simulation which is based on a MINIBALL simulation package [19]. The simulation is used to compare different design options for the T-REX setup, to determine the efficiency of the various cuts necessary in the analysis of the experimental data, to study the contribution of different factors to the observed excitation energy resolution (see table 2), and to support proposals for new experiments with T-REX.

The simulation includes the full T-REX setup and MINIBALL as shown in fig. 9.

An event generator was implemented that generates the ejectiles, recoils, and γ-rays of transfer reactions ac-

Table 2. Contributions from different features to the excitation energy resolution determined by Geant4 simulations. The contributions depend on the beam used, the values reported are for the d(^{22}Ne, p)^{23}Ne/d(^{30}Mg, p)^{31}Mg reaction, both at 2.85 MeV u^{-1}. The 12 μm thick Mylar^{TM} foils in front of the forward barrel detectors contribute only on the order of 1 keV to the final resolution.

Feature	Amount	Excitation energy resolution (FWHM) [keV]	
		Forward	Backward
Detector res.	100 keV	93 / 76	130 / –
Beam spot size	5 mm	120 / 81	40 / –
Target thickness	1 mg cm^{-2}	597 / 497	489 / –
	100 μg cm^{-2}	86 / 29	28 / –
ϑ_{lab} res.	2° to 6°	357 / 315	129 / –
Total res.	1 mg cm^{-2}	680 / 619	399 / –
	100 μg cm^{-2}	137 / 111	150 / –

cording to the user defined angular distributions and/or α-, β-, and γ-sources.

The data output format of the simulation is the same as the output of the calibration program, so that the output of the simulation can be used as input for the particle identification, energy loss calculations, and the reconstruction of the ejectiles to verify the analysis and determine as mentioned above the efficiency of cuts applied in this stage.

8 Excitation energy resolution

The total excitation energy resolution is influenced by multiple contributions: the intrinsic energy resolution of the detectors, the target thickness, the thickness of the screening foils, the beam spot size, and the ϑ_{lab} resolution. The effect that each contribution has on the total excitation energy resolution was determined by comparing the excitation energy resolution of a simulation with all contributions set to zero with that of a simulation where only one of the contributions is non-zero (bottom-up approach). Since the different contributions are not independent the square root of the sum of squares of the effects can be larger than the total excitation energy resolution of the simulation.

Table 2 shows the results of the simulations for the d(^{22}Ne, p)^{23}Ne and the d(^{30}Mg, p)^{31}Mg reactions at 2.85 MeV u^{-1}. For the d(^{22}Ne, p)^{23}Ne reaction results are shown both for the forward and backward detectors, while for the d(^{30}Mg, p)^{31}Mg reaction only results for the forward detectors are shown as the energy of the protons is too low in backward direction. All simulations assume a transfer reaction into the ground state of ^{23}Ne and ^{31}Mg, respectively, with an isotropic angular distribution of the protons in the cm system. The simulations show that the 12 μm thick Mylar^{TM} foils in front of the forward barrel detectors contribute only in the order of a few keV to the final resolution.

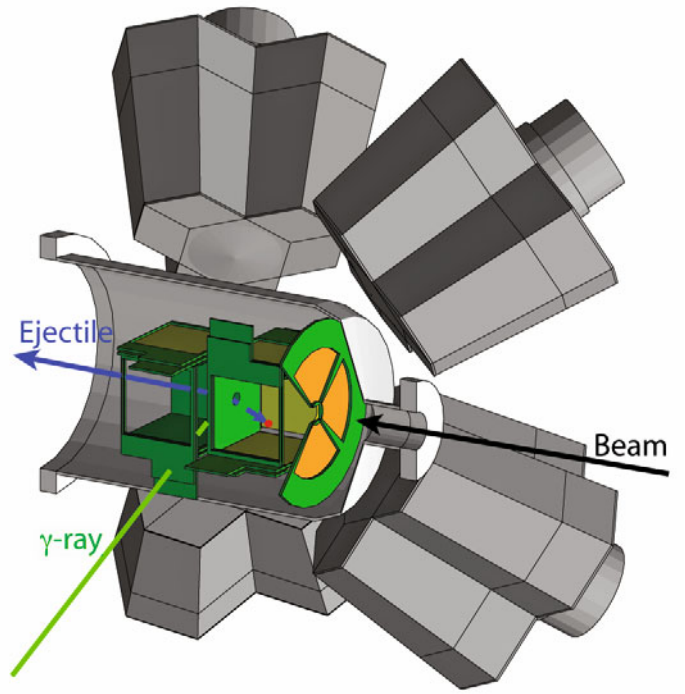


Fig. 9. (Color online) The Geant4 simulation of the T-REX setup from 2008, showing a single transfer event with positive particles in blue, γ-rays in green, and electrons (from ionization processes in the backward barrel detector) in red. The left side of the MINIBALL array, vacuum chamber, and particle detectors is cut away for visualization purposes.

9 Performance

Stable ^{22}Ne beam impinging on a deuterated poly-ethylene target of 1 mg cm^{-2} has been used before each T-REX campaign to test the whole experimental setup and the data analysis, provide additional data for the energy calibration of the silicon detectors, and to improve the determination of the ϑ_{lab} angles of the MINIBALL detectors using the doppler shift of γ-rays emitted by the ^{23}Ne ejectiles. This data also provides an insight into the performance of T-REX.

Figure 10 shows the angular distribution of elastically scattered deuterons. The data was normalized using the luminosity obtained by comparison with a DWBA calculation using optical model parameters that were fitted to reproduce the observed angular distribution. Also shown in the same figure is a DWBA calculation using a set of global optical model parameters taken from [20]. The global parameter set does not reproduce the observed angular distribution very well, which might be attributed to the fact that these parameters (like all global parameter sets) were fitted to transfer data taken at higher beam energies than the 2.85 MeV u^{-1} used in this experiment (for details, see [13]).

Figure 11 shows the background subtracted excitation energy spectrum of the d(^{22}Ne, p)^{23}Ne reaction with cuts on 1017 keV γ-rays (solid black). The γ-rays are emitted in the depopulation of the $1/2^+$ level at 1017 keV as shown

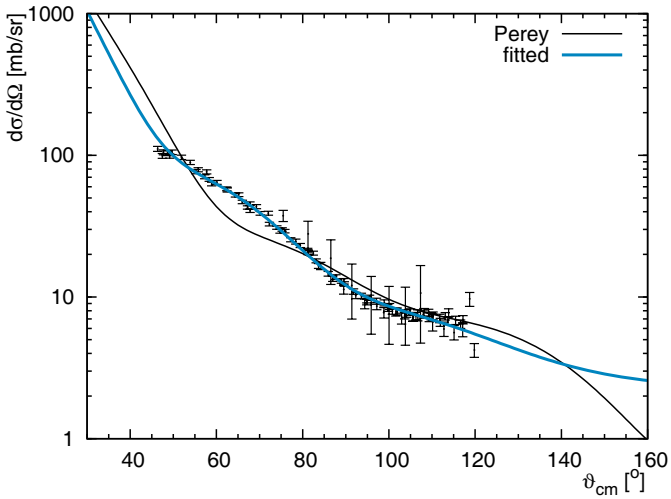


Fig. 10. (Color online) Angular distribution of elastically scattered deuterons from the d(^{22}Ne, d)^{22}Ne reaction with the luminosity determined by a DWBA calculation with optical model parameters fitted to reproduce the data (shown in blue). Shown in black is a DWBA calculation using a global optical model parameter set from [20].

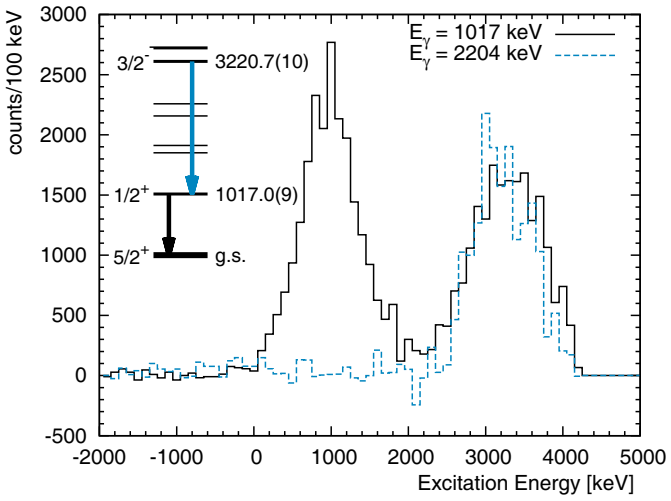


Fig. 11. (Color online) Background subtracted excitation energy spectrum of the d(^{22}Ne, p)^{23}Ne reaction with cuts on the 1017 keV (black) and the 2204 keV (dashed blue) γ-ray. The spectra are corrected for the γ-efficiency and the branching, showing that most of the strength at 3.3 MeV stems from the 3221 keV state. The inset shows the partial level scheme of ^{23}Ne.

in the inset of fig. 11. This level is populated not only directly by the ^{22}Ne reaction but also fed by a higher-lying states around 3.3 MeV. Figure 11 also shows the observed excitation energy spectrum when cutting on 2204 keV γ-rays (dashed blue) showing that most of the strength at 3.3 MeV stems from a $3/2^-$ state at 3221 keV.

The observed excitation energy resolution for the levels at 1017 keV and 3221 keV is 917 keV and 1064 keV, respectively. This excitation energy resolution is larger than that of the simulation, indicating that the effects of some of the contributions were underestimated in the simulation.

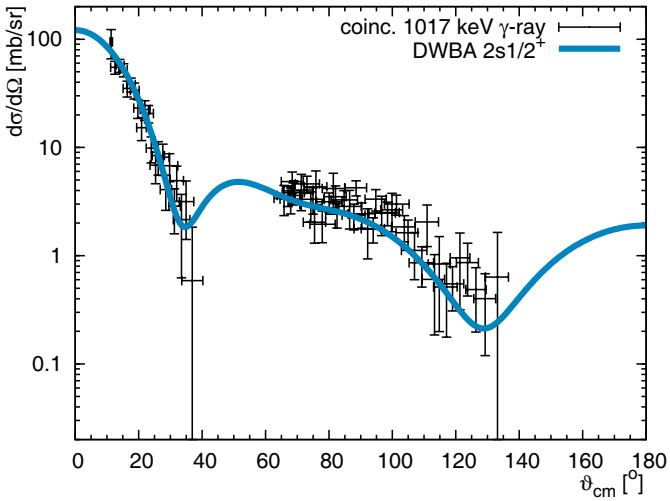


Fig. 12. Angular distribution of protons from the 1017 keV state populated in the d(^{22}Ne, p)^{23}Ne reaction at 2.85 MeV u^{-1}. Shown is the data scaled with the luminosity obtained from the elastically scattered deuterons and the DWBA calculation based on optical model parameters that were fitted to the elastic scattering data.

Figure 12 shows the typical angular distribution measured with T-REX for the d(^{22}Ne, p)^{23}Ne reaction populating the $1/2^+$ level at 1017 keV. Cuts have been applied on both the energy of coincident γ-rays and the reconstructed excitation energy of the ^{23}Ne nucleus. The data is shown together with a DWBA calculation for an orbital momentum transfer $\Delta l = 0$, using the optical model parameters that were fitted to the elastically scattered protons and deuterons. No corrections for particle-γ correlations have been applied.

10 Summary and outlook

The T-REX setup provides a versatile tool for experiments using transfer reactions in inverse kinematics to study the radioactive nuclei provided by the REX-ISOLDE facility. T-REX can also be used for Coulomb excitation experiments, but that is not discussed in this paper. It has been installed at the REX-ISOLDE facility and has been used in several radioactive beam transfer experiments.

The experimental campaign using T-REX will continue for several years and will benefit from the ongoing improvements to the setup.

Furthermore the T-REX setup will gain from the upcoming improvements to the ISOLDE facility in the framework of the HIE-ISOLDE project. The HIE-ISOLDE project will replace the existing REX accelerator by a superconducting linear accelerator that will provide beam energies of up to 5.5 MeV u^{-1} in the first stage and up to 10 MeV u^{-1} in the second stage [21]. T-REX will benefit in multiple ways from the higher beam energy: it will greatly increase the range of radioactive beams accessible for transfer experiments toward higher masses, it will result in more pronounced angular distributions for all

masses, and it will also allow the use of other reactions such as (^{3}He, d) or (^{3}He, α). HIE-ISOLDE will also allow the possibility of installing a 0° mass spectrometer which would identify the ejectiles and thus provide much cleaner spectra.

We thank the MINIBALL and T-REX Collaborations for the support and fruitful discussions during the design phase and the experiments. The latter would not have been possible without the tremendous help from the ISOLDE group. We want to express our gratitude to Michael Böhmer and Ludwig Maier who helped with the design and testing of the custom PCBs and the electronic for the beam diagnostic detectors. We also want to thank Sonja Winkler who bonded and repaired our detectors and Rudi Lutter who wrote and maintained the DAQ for all MINIBALL experiments. The present work is lead by the Technische Universität München and the Katholieke Universiteit Leuven supported by BMBF 06MT238, 06MT9156, DFG Cluster of Excellence "Origin of the Universe" (EXC 153), and the EU through RII3-EURONS (contract no. 506065). This work was also supported by FWO-Vlaanderen (Belgium), by GOA/2004/03 (BOF-KU Leuven) and by the IUAP - Belgian State Belgian Science Policy - (BriX network P6/23). Additional support for the setup came from the University of Edinburgh, CSNSM Orsay, and the Technische Universität Darmstadt (BMBF 06DA9036I).

References

1. R. Hertenberger, H. Kader, F. Merz, F. Eckle, G. Eckle, P. Schiemenz, H. Wessner, G. Graw, Nucl. Instrum. Methods Phys. Res. A **258**, 201 (1987).
2. P.V. Duppen, K. Riisager, J. Phys. G: Nucl. Part. Phys. **38**, 024005 (2011).
3. J. Eberth, G. Pascovici, H. Thomas, N. Warr, D. Weisshaar, D. Habs, P. Reiter, P. Thirolf, D. Schwalm, C. Gund *et al.*, Prog. Part. Nucl. Phys. **46**, 389 (2001).
4. W.N. Catford, C.N. Timis, R.C. Lemmon, M. Labiche, N.A. Orr, L. Caballero, R. Chapman, M. Freer, M. Chartier, H. Savajols *et al.*, J. Phys. G: Nucl. Part. Phys. **31**, S1655 (2005).
5. M. Labiche, W. Catford, R. Lemmon, C. Timis, R. Chapman, N. Orr, B. Fernández-Domínguez, G. Moores, N. Achouri, N. Amzal *et al.*, Nucl. Instrum. Methods Phys. Res. A **614**, 439 (2010) ISSN 0168-9002.
6. C.A. Diget, S.P. Fox, A. Smith, S. Williams, M. Porter-Peden, L. Achouri, P. Adsley, H. Al-Falou, R.A.E. Austin, G.C. Ball *et al.*, JINST **6**, P02005 (2011).
7. S. Pain, J. Cizewski, R. Hatarik, K. Jones, J. Thomas, D. Bardayan, J. Blackmon, C. Nesaraja, M. Smith, R. Kozub *et al.*, Nucl. Instrum. Methods Phys. Res. B **261**, 1122 (2007) ISSN 0168-583X.
8. REX-ISOLDE Collaborations and MINIBALL Collaborations (T. Kröll, V. Bildstein, K. Wimmer, R. Krücken, R. Gernhäuser, R. Lutter, W. Schwerdtfeger, P. Thirolf, B. Bastin, N. Bree *et al.*), AIP Conf. Proc. **1165**, 363 (2009).
9. E. Kugler, Hyperfine Interact. **129**, 23 (2000).
10. U. Köster, V.N. Fedoseyev, A.N. Andreyev, U.C. Bergmann, R. Catherall, J. Cederkäll, M. Dietrich, H. De Witte, D.V. Fedorov, L. Fraile *et al.*, Nucl. Instrum. Methods B **204**, 347 (2003).
11. J. van de Walle, N. Warr, M. Albers, F. Ames, B. Bastin, C. Bauer, V. Bildstein, A. Blazhev, S. Bönig, N. Bree *et al.*, to be submitted to Eur. Phys. J. A.
12. K. Wimmer, T. Kröll, R. Krücken, V. Bildstein, R. Gernhäuser, B. Bastin, N. Bree, J. Diriken, P.V. Duppen, M. Huyse *et al.*, Phys. Rev. Lett. **105**, 252501 (2010).
13. V. Bildstein, Dissertation, TU München (2010) `http://mediatum2.ub.tum.de/node?id=1002184`.
14. A. Ostrowski, S. Cherubini, T. Davinson, D. Groombridge, A. Laird, A. Musumarra, A. Ninane, A. di Pietro, A. Shotter, P. Woods, Nucl. Instrum. Methods A **480**, 448 (2002).
15. *Micron Semiconductor Ltd.*, `http://www.micronsemiconductor.co.uk/`.
16. *Diamond Materials*, `http://www.diamond-materials.com`.
17. *mesytec GmbH & Co. KG*, `http://www.mesytec.com/`.
18. S. Agostinelli, J. Allison, K. Amako, J. Apostolakis, H. Araujo, P. Arce, M. Asai, D. Axen, S. Banerjee, G. Barrand *et al.*, Nucl. Instrum. Methods A **506**, 250 (2003).
19. H.H. Boie, Dissertation, Universität Heidelberg (2009) `http://www.ub.uni-heidelberg.de/archiv/9535`.
20. C.M. Perey, F.G. Perey, At. Data Nucl. Data Tables **17**, 1 (1976).
21. M. Lindroos, P. Butler, M. Huyse, K. Riisager, Nucl. Instrum. Methods B **266**, 4687 (2008).